Journal of Astronomical Telescopes, Instruments, and Systems

AstronomicalTelescopes.SPIEDigitalLibrary.org

Transiting Exoplanet Survey Satellite

George R. Ricker
Joshua N. Winn
Roland Vanderspek
David W. Latham
Gáspár Á. Bakos
Jacob L. Bean
Zachory K. Berta-Thompson
Timothy M. Brown
Lars Buchhave
Nathaniel R. Butler
R. Paul Butler
William J. Chaplin
David Charbonneau
Jørgen Christensen-Dalsgaard
Mark Clampin
Drake Deming
John Doty
Nathan De Lee

SPIE.

Downloaded From: https://www.spiedigitallibrary.org/journals/Journal-of-Astronomical-Telescopes,-Instruments,-and-Systems on 12/10/2018
Terms of Use: https://www.spiedigitallibrary.org/terms-of-use

Journal of Astronomical Telescopes, Instruments, and Systems 1(1), 014003 (Jan–Mar 2015)

Transiting Exoplanet Survey Satellite

George R. Ricker,[a,*] Joshua N. Winn,[a] Roland Vanderspek,[a] David W. Latham,[b] Gáspár Á. Bakos,[c] Jacob L. Bean,[d] Zachory K. Berta-Thompson,[a] Timothy M. Brown,[e] Lars Buchhave,[b,f] Nathaniel R. Butler,[g] R. Paul Butler,[h] William J. Chaplin,[i,j] David Charbonneau,[b] Jørgen Christensen-Dalsgaard,[j] Mark Clampin,[k] Drake Deming,[l] John Doty,[m] Nathan De Lee,[n,o] Courtney Dressing,[b] Edward W. Dunham,[p] Michael Endl,[q] Francois Fressin,[b] Jian Ge,[r] Thomas Henning,[s] Matthew J. Holman,[b] Andrew W. Howard,[t] Shigeru Ida,[u] Jon M. Jenkins,[v] Garrett Jernigan,[w] John Asher Johnson,[b] Lisa Kaltenegger,[s] Nobuyuki Kawai,[u] Hans Kjeldsen,[j] Gregory Laughlin,[x] Alan M. Levine,[a] Douglas Lin,[x] Jack J. Lissauer,[v] Phillip MacQueen,[q] Geoffrey Marcy,[y] Peter R. McCullough,[z,aa] Timothy D. Morton,[c] Norio Narita,[bb] Martin Paegert,[o] Enric Palle,[cc] Francesco Pepe,[dd] Joshua Pepper,[o,ee] Andreas Quirrenbach,[ff] Stephen A. Rinehart,[k] Dimitar Sasselov,[b] Bun'ei Sato,[u] Sara Seager,[a] Alessandro Sozzetti,[gg] Keivan G. Stassun,[o,hh] Peter Sullivan,[a] Andrew Szentgyorgyi,[b] Guillermo Torres,[b] Stephane Udry,[dd] and Joel Villasenor[a]

[a]Massachusetts Institute of Technology, 77 Massachusetts Avenue, Cambridge, Massachusetts 02139, United States
[b]Harvard-Smithsonian Center for Astrophysics, Cambridge, Massachusetts 02138, United States
[c]Princeton University, Princeton, New Jersey 08540, United States
[d]University of Chicago, Chicago, Illinois 60611, United States
[e]Las Cumbres Observatory Global Telescope, Goleta, California 93117, United States
[f]University of Copenhagen, 1165 Copenhagen, Denmark
[g]Arizona State University, Tempe, Arizona 85004, United States
[h]Carnegie Institute of Washington, Department of Terrestrial Magnetism, Washington, DC 20015, United States
[i]University of Birmingham, Birmingham B15 2TT, United Kingdom
[j]Aarhus University, Stellar Astrophysics Centre, 8000 Aarhus, Denmark
[k]NASA Goddard Space Flight Center, Green Belt, Maryland 20771, United States
[l]University of Maryland, College Park, Maryland 20742, United States
[m]Noqsi Aerospace, Ltd., Pine, Colorado 80470, United States
[n]Northern Kentucky University, Highland Heights, Kentucky 41099, United States
[o]Vanderbilt University, Nashville, Tennessee 37235, United States
[p]Lowell Observatory, Flagstaff, Arizona 86001, United States
[q]McDonald Observatory, Austin, Texas 78712, United States
[r]University of Florida, Gainesville, Florida 32611, United States
[s]Max-Planck-Institut für Astronomie, 69117 Heidelberg, Germany
[t]University of Hawaii, Manoa, Hawaii 96822, United States
[u]Tokyo Institute of Technology, Tokyo 152-8851, Japan
[v]NASA Ames Research Center, Mountain View, California 94035, United States
[w]University of California, Space Science Laboratory, Berkeley, California 94720, United States
[x]UCO/Lick Observatory, Santa Cruz, California 95064, United States
[y]University of California, Berkeley, California 94720, United States
[z]Space Telescope Science Institute, Baltimore, Maryland 21218, United States
[aa]Johns Hopkins University, Baltimore, Maryland 21218, United States
[bb]National Astronomical Observatory of Japan, Tokyo 181-8588, Japan
[cc]Instituto de Astrofisica de Canarias, E38205 La Laguna (Tenerife), Spain
[dd]Observatoire de Genève, 1290 Versoix, Switzerland
[ee]Lehigh University, Bethlehem, Pennsylvania 18015, United States
[ff]Landessternwarte, Zentrum für Astronomie der Universität, 69117 Heidelberg, Germany
[gg]INAF–Osservatorio Astrofisico di Torino, 10025 Pino Torinese, Torino, Italy
[hh]Fisk University, Nashville, Tennessee 37208, United States

Abstract. The Transiting Exoplanet Survey Satellite (TESS) will search for planets transiting bright and nearby stars. TESS has been selected by NASA for launch in 2017 as an Astrophysics Explorer mission. The spacecraft will be placed into a highly elliptical 13.7-day orbit around the Earth. During its 2-year mission, TESS will employ four wide-field optical charge-coupled device cameras to monitor at least 200,000 main-sequence dwarf stars with $I_C \approx 4-13$ for temporary drops in brightness caused by planetary transits. Each star will be observed for an interval ranging from 1 month to 1 year, depending mainly on the star's ecliptic latitude. The longest observing intervals will be for stars near the ecliptic poles, which are the optimal locations for follow-up observations with the James Webb Space Telescope. Brightness measurements of preselected target stars will be recorded every 2 min, and full frame images will be recorded every 30 min. TESS stars will be 10 to 100 times brighter than those surveyed by the pioneering Kepler mission. This will make TESS planets easier to characterize with follow-up observations. TESS is expected to find more than a thousand planets smaller than Neptune, including dozens that are comparable in size to the Earth. Public data releases will occur every 4 months, inviting immediate community-wide efforts to study the new planets. The TESS legacy will be a catalog of the nearest and brightest stars hosting transiting planets, which will endure as highly favorable targets for detailed investigations. © *The Authors. Published by SPIE under a Creative Commons Attribution 3.0 Unported License. Distribution or reproduction of this work in whole or in part requires full attribution of the original publication, including its DOI.* [DOI: 10.1117/1.JATIS.1.1.014003]

Keywords: exoplanet; extrasolar planet; photometry; satellite; transits.

Paper 14012P received Jun. 4, 2014; revised manuscript received Aug. 24, 2014; accepted for publication Aug. 25, 2014; published online Oct. 24, 2014.

*Address all correspondence to: George R. Ricker, E-mail: grr@space.mit.edu

Downloaded From: https://www.spiedigitallibrary.org/journals/Journal-of-Astronomical-Telescopes,-Instruments,-and-Systems on 12/10/2018
Terms of Use: https://www.spiedigitallibrary.org/terms-of-use

1 Introduction

The study of exoplanets—planets outside our solar system—is one of the most exciting and rapidly advancing fields of science. Especially valuable are systems in which a planet's orbit carries it directly across the face of its host star. For such a "transiting" planet, it is possible to determine the planet's mass and radius, its orbital parameters, and its atmospheric properties.[1]

Of particular interest are planets with sizes between those of the Earth and Neptune. Little is known about them, because there are no examples in the solar system. NASA's Kepler mission revolutionized exoplanetary science by revealing that such planets are abundant,[2,3] and seem to have a wide range of compositions[4] and interesting orbital configurations.[5] However, most of the Kepler stars are too faint for detailed follow-up observations.

The Transiting Exoplanet Survey Satellite, or TESS, will take the next logical step after Kepler by searching the nearest and brightest stars for transiting planets. The primary objective of TESS is to discover hundreds of transiting planets smaller than Neptune, with host stars bright enough for follow-up spectroscopy to measure planetary masses and atmospheric compositions. This objective will be achieved by conducting a 2-year all-sky survey, during which differential time-series photometry will be performed for hundreds of thousands of stars. The main value of TESS data will not be statistical completeness, but rather the relative ease of following up on discoveries with current and planned instruments.

This paper summarizes the TESS mission: its history (Sec. 2), design considerations (Sec. 3), payload (Sec. 4), spacecraft (Sec. 5), orbit (Sec. 6), operations (Sec. 7), anticipated results (Sec. 8), institutional partners (Sec. 9), and broader context (Sec. 10). Since the TESS mission is still in phase B as of writing, the information presented here is provisional and reflects the design as of mid-2014.

2 History

The initial discussions leading to the TESS concept began at the Massachusetts Institute of Technology (MIT) and the Smithsonian Astrophysical Observatory (SAO) in late 2005. In early 2006, a proposal for a Mission of Opportunity was submitted to NASA to use the optical camera of the High Energy Transient Explorer[6] to perform a survey for transiting planets. This proposal was not selected.

Later in 2006 and early 2007, TESS was reformulated as a standalone small mission. Seed funding was obtained from private individuals, the Kavli Foundation, Google, MIT, the SAO, and the NASA Ames Research Center, but attempts to raise the funds required for a full mission were not successful.

In 2008, TESS was reconceived as a Small Explorer Mission (SMEX), a NASA program with a cost cap of $100m. The TESS SMEX proposal was funded for a phase A study during 2008 to 2009, but was not chosen to proceed into phase B.

During the next 2 years, the TESS concept was gradually refined, and a new proposal was submitted to the NASA Explorer program in 2011. The larger cost cap ($200m) enabled several key improvements, particularly the use of a high-Earth elliptical orbit, which provides a more stable platform for precise photometry than the low-Earth orbit that had been the basis of all the previous proposals. TESS was selected by NASA for a phase A study as an Explorer mission in Fall 2011, and proceeded to phase B in April 2013.

3 Design Considerations

This section describes some of the considerations that led to the current design of the TESS mission.

3.1 *Sky Coverage*

Although many transiting planets have been found, relatively few of them orbit stars bright enough to enable follow-up measurements of planet masses and atmospheres. Therefore, a prime objective of TESS is to monitor bright stars. Since the brightest stars are nearly evenly distributed over the entire sky, this desire led in the direction of an all-sky survey.

3.2 *Period Sensitivity*

Ideally, the mission would detect planets with a broad range of orbital periods, with P_{min} near the Roche limit of a few hours, and P_{max} of a year or longer. However, the choice of P_{max} determines the mission duration and thereby has a disproportionate influence on cost. Furthermore, transit surveys are strongly and inherently biased toward short periods. (As shown in Refs. 7 and 8, in an idealized imaging survey limited only by photon-counting noise, the effective number of stars that can be searched for transiting planets of period P varies as $P^{-5/3}$.) Indeed, the period distribution of Kepler detections[2] reaches a maximum at $\approx$10 days, taking into account the period dependencies of both the transit detection efficiency and the occurrence of planets. Hence, even a value of P_{max} as short as 10 days should yield many discoveries.

Choosing P_{max} as short as 10 days rules out the detection of habitable-zone planets around Sun-like stars. However, it is possible to gain access to habitable-zone planets around M stars if at least a portion of the sky is observed with $P_{\mathrm{max}} \gtrsim 40$ days. (For an M0 star with $T_{\mathrm{eff}} = 3800$ K, the range of orbital distances receiving a bolometric insolation within a factor of two of the Earth's insolation corresponds roughly to $P = 25$–75 days.) And if there is a portion of the sky to be searched more extensively, it would be advantageous for that portion to coincide with the zones of longest continuous visibility with the James Webb Space Telescope (JWST), which will likely be the best telescope for follow-up studies of planetary atmospheres. Those zones are centered on the ecliptic poles.[9]

Together these considerations led to the choices of $P_{\mathrm{max}} \approx 10$ days in general, and $P_{\mathrm{max}} \gtrsim 40$ days for as large an area as possible surrounding the ecliptic poles.

3.3 *Type of Stars Monitored*

While it would be interesting to survey all types of stars, it is logical to concentrate on main-sequence dwarfs with spectral types F5 to M5. Evolved stars and early-type dwarfs are large, inhibiting the detection of small planets. Dwarfs with spectral types earlier than F5 also rotate rapidly, broadening their spectral lines and preventing precise radial-velocity (PRV) monitoring.

On the other side of the spectral sequence, M dwarfs are especially attractive targets. They are abundant: about three-quarters of the stars in the solar neighborhood are M0–M5 dwarfs. They are relatively unexplored for transiting planets, because they constituted only a small minority of the Kepler target list. Furthermore, the transit signal of a small planet is easier to detect for an M dwarf than it would be for a larger star of the same apparent magnitude, facilitating both planet

Downloaded From: https://www.spiedigitallibrary.org/journals/Journal-of-Astronomical-Telescopes,-Instruments,-and-Systems on 12/10/2018
Terms of Use: https://www.spiedigitallibrary.org/terms-of-use

discovery and follow-up observations with JWST and other telescopes.

However, stars with spectral types later than M5 are rarer and optically faint. They could be observed advantageously at near-infrared wavelengths, but this would greatly increase the mission's cost, complexity, and risk. Furthermore, planets transiting the very latest-type stars can be detected with ground-based instruments, as demonstrated by the MEarth survey.[10] For these reasons, the F5–M5 range of spectral types was considered to be most important for TESS.

3.4 *Detector and Bandpass*

The best astronomical detectors in the optical band are silicon charge-coupled devices (CCDs), which have excellent linearity and dynamic range for bright objects, and a long spaceflight heritage. A wide bandpass is preferred to reduce photon-counting noise. However, very wide bands present challenges in constructing a wide-field and well-focused optical system. Enhanced sensitivity to red wavelengths is desired because small planets are more easily detected around small stars, which are cool and red.

These considerations led to the choice of a 600 to 1000 nm bandpass. The red end represents the red limit of silicon CCD sensitivity, and the width of 400 nm was the largest practical choice for the optical design. This bandpass is centered on the traditional I_C band but is much wider (see Fig. 1). It is comparable to the union of the R_C, I_C, and z bands.

3.5 *Number of Stars Monitored*

Kepler's transit detection rate[2] for "super-Earths" ($1.25 - 2\,R_\oplus$) with $P < 10$ days was about 0.2%. This represents the product of the occurrence rate (~5%) and the geometric transit probability (~5%). Therefore, TESS needs to monitor at least 500 stars for each super-Earth detection. The desire to find hundreds of such planets leads to the requirement to monitor $\gtrsim 10^5$ stars.

According to Galactic star count models,[11] the brightest 10^5 dwarf stars have a limiting apparent magnitude of $I_C \approx 10$. In fact, the TESS design employs a larger catalog ($\gtrsim 2 \times 10^5$ stars) selected according to transit detectability rather than strictly on apparent magnitude. This leads to a limiting magnitude of $I_C \lesssim 10 - 13$, depending on spectral type. The faint M dwarfs, for example, have such small sizes that they can still be usefully searched for small planets.

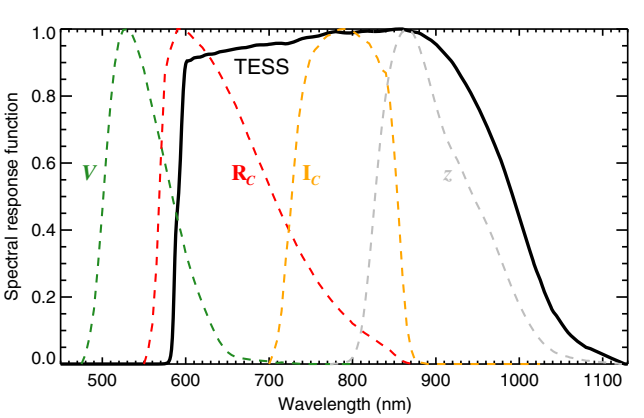

Fig. 1 The Transiting Exoplanet Survey Satellite (TESS) spectral response function (black line), defined as the product of the long-pass filter transmission curve and the detector quantum efficiency curve. Also plotted, for comparison, are the Johnson–Cousins V, R_C, and I_C filter curves and the Sloan Digital Sky Survey z filter curve. Each of the functions has been scaled to have a maximum value of unity.

3.6 *Aperture Size*

Stars must be monitored with sufficient photometric precision to detect planetary transits. This leads to requirements on the collecting area and other properties of the cameras, although the derivation of those requirements is not straightforward because of the wide variation in the characteristics of the transit signals. As reviewed in Ref. 1, the transit depth varies with the radii of the star ($R_\star$) and planet (R_p)

$$\delta = (337\ \text{ppm}) \left(\frac{R_p}{2\,R_\oplus}\right)^2 \left(\frac{R_\star}{R_\odot}\right)^{-2}, \tag{1}$$

and the transit duration (T) depends on the stellar mean density ($\rho_\star$) as well as the orbital period (P) and dimensionless transit impact parameter (b)

$$T = (3.91\ \text{h}) \left(\frac{\rho_\star}{\rho_\odot}\right)^{-1/3} \left(\frac{P}{10\ \text{days}}\right)^{1/3} \sqrt{1 - b^2}. \tag{2}$$

In these equations, the fiducial case is a transiting planet with $R_p = 2\,R_\oplus$ in a 10-day circular orbit around a Sun-like star ($R_\star = R_\odot$, $\rho = \rho_\star$).

Monte Carlo simulations were performed[12] to establish the requirements for detecting a certain number of transiting planets, taking into account the likely distribution of stellar apparent magnitudes and radii; the occurrence of planets of various sizes and orbits; as well as noise due to sky background, instrumental readout, and other sources. The results of this study, summarized in Sec. 8, indicate that detecting hundreds of super-Earths requires ≈50 cm^2 of effective collecting area (i.e., the actual collecting area multiplied by all throughput factors including transmission losses and quantum efficiency). This corresponds to an effective aperture diameter of $D \approx 10$ cm.

3.7 *Time Sampling*

Since the typical transit durations are measured in hours, the time sampling of the photometric observations should be substantially less than an hour. The timescale of the partial transit phases (ingress and egress) is $\sim T(R_p/R_\star)$, which is typically several minutes for planets smaller than Neptune. Therefore, to avoid excessive smearing of the partial transit signals, a time sampling of a few minutes or shorter is preferred. For TESS, the brightness measurements of the preselected stars will be recorded every 2 min or shorter, which is consistent with these requirements and also enables asteroseismology (see Sec. 8.3).

3.8 *Orbit*

The ideal orbit for the TESS spacecraft would allow for continuous observations lasting for weeks, and would be stable to perturbations over the multiyear duration of the survey. It would offer a low-radiation environment, to avoid high trapped-particle fluxes and resulting degradation of the CCDs and flight electronics. It would also offer a stable thermal environment and minimal attitude disturbance torques, to provide a stable

Downloaded From: https://www.spiedigitallibrary.org/journals/Journal-of-Astronomical-Telescopes,-Instruments,-and-Systems on 12/10/2018
Terms of Use: https://www.spiedigitallibrary.org/terms-of-use

platform for precise photometry. The orbit would be achievable with a moderate ΔV, avoiding the need for a costly secondary propulsion unit. Furthermore, to facilitate data transfer, the spacecraft would be close to the Earth during at least a portion of the orbit. As explained in Sec. 6, these requirements were met by choosing an elliptical orbit around the Earth, with approximate perigee and apogee distances of 17 and 59 $R_{\oplus}$, and a period of 13.7 days.

4 Payload

The TESS payload consists of four identical cameras and a data handling unit (DHU). Each camera consists of a lens assembly with seven optical elements, and a detector assembly with four CCDs and their associated electronics. All four cameras are mounted onto a single plate. These components will now be discussed in turn.

4.1 *Lens Assembly*

Each of the four identical TESS lenses is an $f/1.4$ custom design consisting of seven optical elements, with an entrance pupil diameter of 10.5 cm (see Figs. 2 and 3 and Table 1). For ease of manufacture, all lens surfaces are spherical except for two mild aspheres. There are two separate aluminum lens barrels that are fastened and pinned together. All optical elements have antireflection coatings. The surface of one element also has a long-pass filter coating to enforce the cutoff at 600 nm. The red limit at 1000 nm is set by the quantum-efficiency curve of the CCDs (see Fig. 1).

Each lens forms a 24 deg $\times$ 24 deg unvignetted image on the four-CCD mosaic in its focal plane. The optical design was optimized to provide small image spots of a consistent size across the field of view (FOV), and produce undersampled images similar to those of Kepler.[13] At nominal focus and flight temperature (-75°C), the 50% ensquared-energy half-width is 15 μm (1 pixel or 0.35 arc min) averaged over the FOV. Each lens is equipped with a lens hood, which reduces the effects of scattered light from the Earth and Moon.

4.2 *Detector Assembly*

The focal plane consists of four back-illuminated MIT/Lincoln Laboratory CCID-80 devices. Each CCID-80 consists of a 2048×2048 imaging array and a 2048×2048 frame-store region, with 15×15 μm pixels. The frame-store region allows rapid shutterless readout ($\approx$4 ms). On each CCD there are four regions of 512 columns, each of which has a dedicated output register. The full well capacity is approximately 200,000 electrons. The four CCDs are abutted with a 2-mm gap, creating an effective 4096×4096 imaging array contained within a 62 mm $\times$ 62 mm square (see Fig. 3).

The CCDs have an operational temperature of -75°C to reduce the dark current to a negligible level. They are read out at 625 kHz and the read noise is $<10\,e^{-}$. The detector electronics are packaged onto two compact double-sided printed circuit boards, each 12 cm in diameter, which are located beneath the CCD focal plane and transmit digitized video data over a serial LVDS link to a DHU.

4.3 *Data Handling Unit*

The TESS DHU is a Space Micro Image Processing Computer (IPC-7000) which consists of six boards: an IPC, which contains two Virtex-7 field-programmable gate arrays (FPGAs) that serve as interfaces to the four cameras and perform high-speed data processing; a Proton 400K single board computer, which is responsible for commanding, communicating with the spacecraft master avionics unit, and interfacing with the Ka-band transmitter; two 192 GB solid-state buffer (SSB) cards for

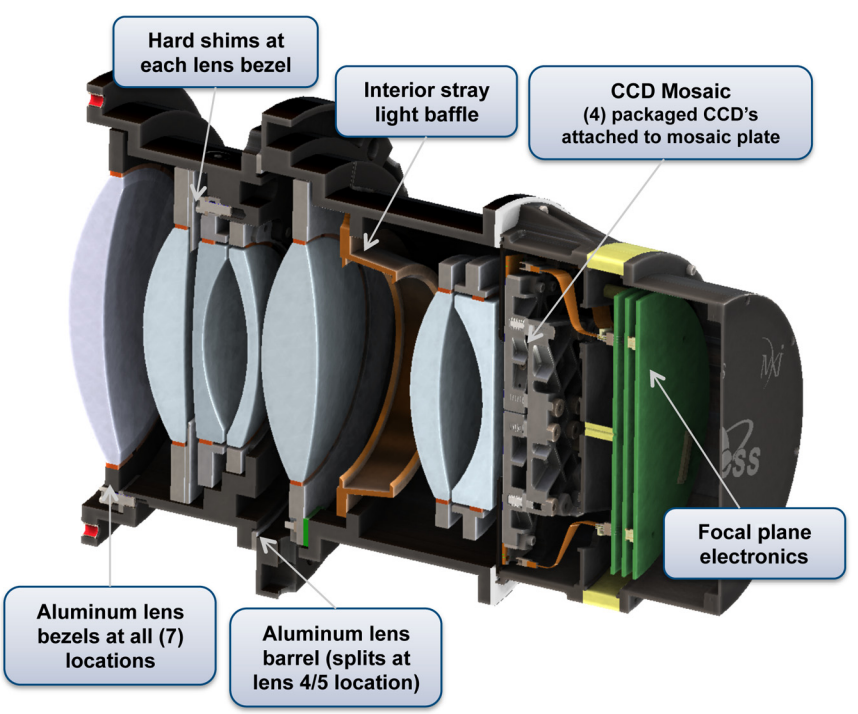

Fig. 2 Diagram of the lens assembly, charge-coupled device (CCD) focal plane, and detector electronics for one of the four TESS cameras.

Downloaded From: https://www.spiedigitallibrary.org/journals/Journal-of-Astronomical-Telescopes,-Instruments,-and-Systems on 12/10/2018
Terms of Use: https://www.spiedigitallibrary.org/terms-of-use

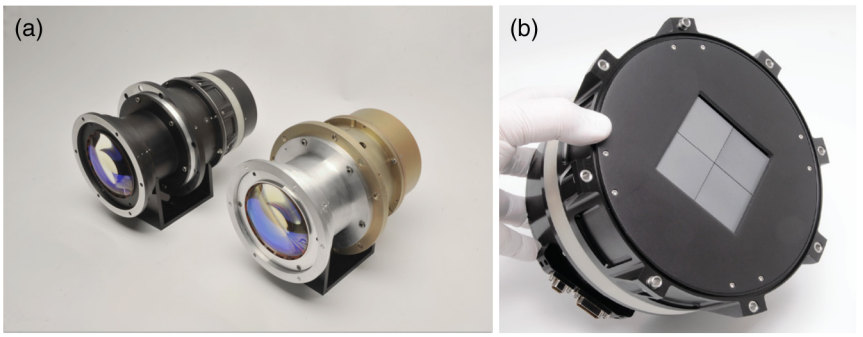

Fig. 3 (a) Two lens prototypes were constructed during phase A. One was subjected to thermal vacuum testing at the operational temperature; the other was subjected to vibration testing. (b) The detector assembly of one of the prototype lenses. The frame-store regions of the CCDs are covered.

Table 1 Characteristics of the TESS lenses. Ensquared energy is the fraction of the total energy of the point-spread function that is within a square of the given dimensions centered on the peak.

Field of view of each lens	24 deg × 24 deg
Combined field of view	24 deg × 96 deg = 2300 deg^2
Entrance pupil diameter	10.5 cm
Focal ratio (f/#)	f/1.4
Wavelength range	600 to 1000 nm
Ensquared energy	50% within 15 × 15 μm (1 pixel, or 0.35 × 0.35 arc min)
	90% within 60 × 60 μm (4 × 4 pixels or 1.4 × 1.4 arc min)

mass data storage; an analog I/O power switch board to control instrument power; and a power supply board for the DHU.

The CCDs produce a continuous stream of images with an exposure time of 2 s. These are received by the FPGAs on the IPC, and summed into consecutive groups of 60, giving an effective exposure time of 2 min. During science operations, the DHU performs real-time processing of data from the four cameras, converting CCD images into the data products required for ground postprocessing. A primary data product is a collection of subarrays (nominally 10 × 10 pixels) centered on preselected target stars. The Proton 400 K extracts these subarrays from each 2 min summed image, compresses them, and stores them in the SSB prior to encapsulation as CCSDS packets for the Ka-band transmitter. Full frame images (FFIs) are also stacked every 30 min and stored in the SSB. Data from the SSB are downlinked every 13.7 days at perigee.

5 Spacecraft

TESS uses the orbital LEOStar-2/750 bus equipped with a Ka-band transmitter and a monopropellant (hydrazine) propulsion system. The bus has a three-axis controlled, zero-momentum attitude control system, and two deployed solar array wings. The total observatory power draw is estimated to be 290 W, and the solar arrays are capable of producing 415 W.

To achieve fine pointing, the spacecraft uses four reaction wheels and high-precision quaternions produced by the science cameras. The transmitter has a body-fixed high-gain antenna with a diameter of 0.7 m, a power of 2 W, and a data rate of 100 Mb s^{-1}. This is sufficient to downlink the science data during 4-h intervals at each perigee.

The cameras are bolted onto a common plate that is attached to the spacecraft, such that their FOV are lined up to form a rectangle measuring 24 deg × 96 deg on the sky (see Figs. 4 and 7). Four elliptical holes in the plate allow shimless alignment of the four cameras at the desired angles.

6 Orbit

The TESS orbit is elliptical, with nominal perigee and apogee of 17 $R_\oplus$ and 59 $R_\oplus$, and a 13.7-day period in 2:1 resonance with the Moon's orbit. The TESS orbit is inclined from the ecliptic plane, thereby eliminating lengthy eclipses by the

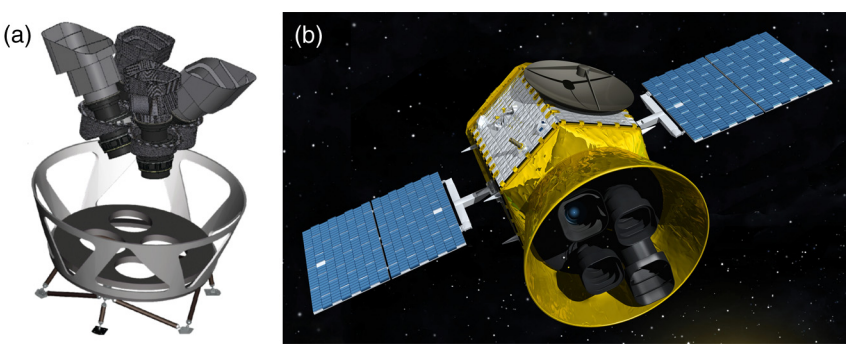

Fig. 4 (a) Diagram illustrating the orientations of the four TESS cameras, lens hoods, and mounting platform. (b) Artist's conception of the TESS spacecraft and payload.

Downloaded From: https://www.spiedigitallibrary.org/journals/Journal-of-Astronomical-Telescopes,-Instruments,-and-Systems on 12/10/2018
Terms of Use: https://www.spiedigitallibrary.org/terms-of-use

Earth and Moon. The spacecraft orbit is operationally stable as a result of the Moon leading or lagging the spacecraft apogee by ≈90 deg, averaging out the lunar perturbations.[14] The orbit remains above the Earth's radiation belts, leading to a relatively low-radiation environment with a mission total ionizing dose of <1 krad. The nearly constant thermal environment ensures that the CCDs will operate near −75°C, with temperature variations $< 0.1°C\,h^{-1}$ for 90% of the orbit, and $<2°C\,h^{-1}$ throughout the entire orbit.

This orbit can be reached efficiently using a small supplemental propulsion system ($\Delta V \approx 3\ km\,s^{-1}$) augmented by a lunar gravity assist. The specific path to the orbit will depend on the launch date and launch vehicle. In a nominal scenario (illustrated in Fig. 5), TESS is launched from Cape Canaveral into a parking orbit with an equatorial inclination of 28.5 deg. The apogee is raised to 400,000 km after two additional burns by the spacecraft hydrazine system, one at perigee of the first phasing orbit and another at perigee of the second phasing orbit. An adjustment is made at third perigee, before a lunar flyby raises the ecliptic inclination to about 40 deg. A final period-adjust maneuver establishes the desired apogee and the 13.7-day period. The final orbit is achieved about 60 days after launch, and science operations begin soon afterward.

The orbital period and semimajor axis are relatively constant, with long-term exchanges of eccentricity and inclination over a period of order 8 to 12 years (driven by a Kozai-like mechanism[14]). There are also short-term oscillations with a period of 6 months caused by solar perturbations (see Fig. 6). The orbit is stable on the timescale of decades, or more, and requires no propulsion for station-keeping. Table 2 lists a number of advantages of this type of orbit for TESS.

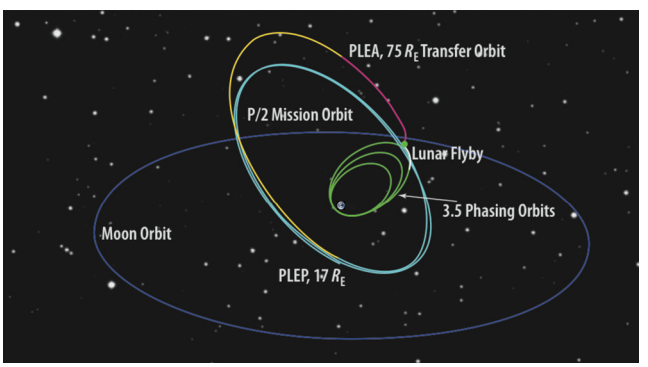

Fig. 5 Maneuvers and scenario for achieving the TESS mission orbit. PLEP is the postlunar-encounter perigee and PLEA is the postlunar-encounter apogee.

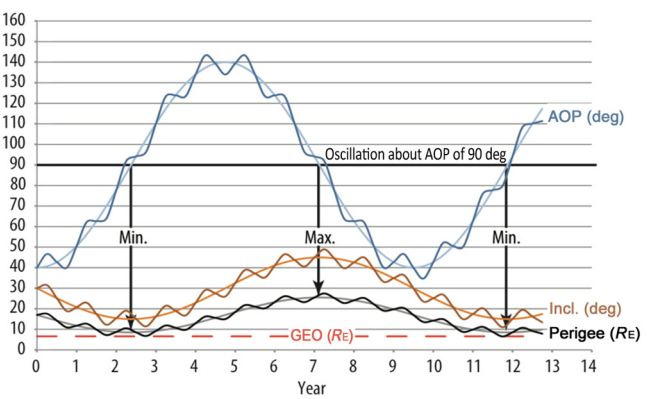

Fig. 6 Calculated time variations in the elements of the nominal TESS mission orbit. The units of each curve are specified in the legend. AOP is the argument of perigee. GEO is the geosynchronous Earth orbit.

Table 2 Characteristics of the TESS spacecraft orbit and comparisons to a low-Earth orbit.

Extended and unbroken observations: >300 h orbit^{-1}
Thermal stability: $< 0.1°C\,h^{-1}$ (passive control)
Earth/Moon stray light: ~10^6 times lower than in low-Earth orbit
Low-radiation levels: no South Atlantic anomaly or outer belt electrons
Frequent launch windows: 20 days per lunation
High data rates at perigee: ~100 Mb s^{-1}
Excellent pointing stability: no drag or gravity gradient torques
Simple operations: single 4-h downlink and repoint every 2 weeks
Long lifetime: several decades above GEO (>6.6 $R_\oplus$)

7 Survey Operations

7.1 *Star Selection*

A catalog of preselected stars will be monitored at a cadence of 2 min or better. Ideally, the catalog will include ≳200,000 main-sequence FGKM stars that are sufficiently bright and small to enable the detection of transiting planets smaller than Neptune. This corresponds to approximately $I_C < 12$ for FGK stars and $I_C < 13$ for M dwarfs.[12] These stars are bright enough that it should be possible to assemble a list using currently available all-sky surveys. A draft catalog has been constructed using the 2MASS,[15] Tycho-2,[16] and UCAC4[17] catalogs, supplemented with smaller catalogs of nearby M dwarfs. For the M stars, infrared magnitudes allow for discrimination between dwarfs and giants.[18] G and K dwarfs are distinguished from giants through their relatively rapid reduced proper motion.[19] It may also be possible to use trigonometric parallaxes measured by the ongoing European "Gaia" mission, if they become available early enough for TESS mission planning. The TESS target catalog will be publicly released prior to launch.

7.2 *Scanning Strategy*

The four cameras act as a 1 × 4 array, providing a combined FOV of 24 deg × 96 deg or 2300 deg^2 (see Fig. 7). The north and south ecliptic hemispheres are each divided into 13 partially overlapping sectors of 24 deg × 96 deg, extending from an ecliptic latitude of 6 deg to the ecliptic pole. Each sector is observed continuously for two spacecraft orbits (27.4 days), with the boresight of the four-camera array pointed nearly anti-solar. After two orbits, the FOV is shifted eastward in ecliptic longitude by about 27 deg, to observe the next sector. Observing an entire hemisphere takes 1 year, and the all-sky survey takes 2 years. (A video illustrating the TESS survey strategy, along with the pathway to the spacecraft orbit, can be seen at http://www.youtube.com/watch?v=mpViVEO-ymc.).

Downloaded From: https://www.spiedigitallibrary.org/journals/Journal-of-Astronomical-Telescopes,-Instruments,-and-Systems on 12/10/2018
Terms of Use: https://www.spiedigitallibrary.org/terms-of-use

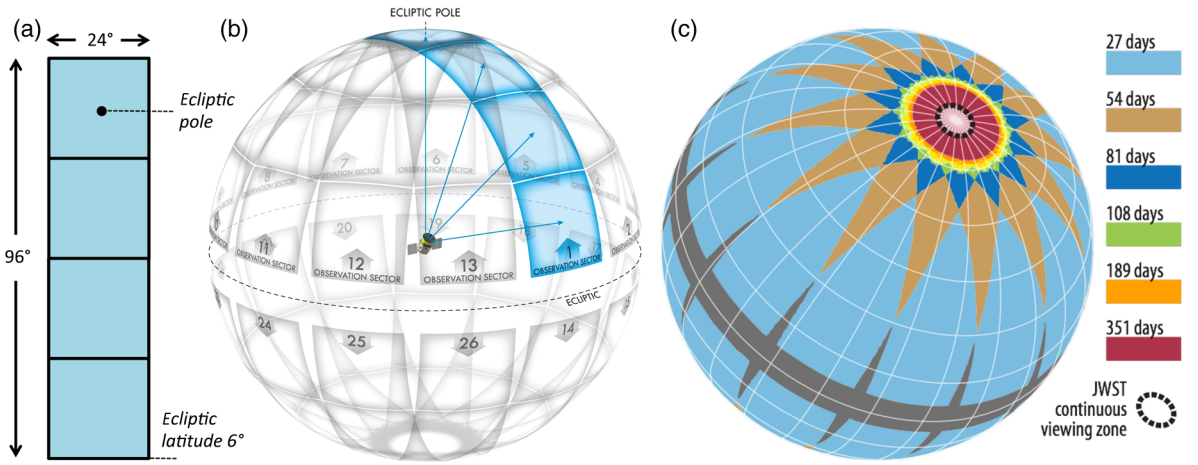

Fig. 7 (a) The instantaneous combined field of view of the four TESS cameras. (b) Division of the celestial sphere into 26 observation sectors (13 per hemisphere). (c) Duration of observations on the celestial sphere taking into account the overlap between sectors. The dashed black circle enclosing the ecliptic pole shows the region which James Webb Space Telescope will be able to observe at any time.

The overlap of the sectors is illustrated in Fig. 7. Approximately 30,000 deg^2 are observed for at least 27 days. Close to the ecliptic poles, approximately 2800 deg^2 are observed for more than 80 days. Surrounding the ecliptic poles, approximately 900 deg^2 are observed for more than 300 days.

7.3 *Data Downlink and Housekeeping Operations*

At perigee, science operations are interrupted for no more than 16 h to point TESS's antenna toward Earth, downlink data, and resume observing. This includes a nominal 4-h period for Ka-band science data downlink using NASA's Deep Space Network. In addition, momentum unloading is occasionally needed due to the ≈1.5 N m of angular momentum build-up induced by solar radiation pressure. For this purpose, TESS uses its hydrazine thrusters.

7.4 *Ground-Based Data Analysis and Follow-Up*

The TESS data will be processed with a data reduction pipeline based on software that was developed for the Kepler mission.[20] This includes pixel-level calibration, background subtraction, aperture photometry, identification and removal of systematic errors, and the search for transits with a wavelet-domain matched filter.

Once the data are processed and transits are identified, selected stars will be characterized with ground-based imaging and spectroscopy. These observations are used to establish reliable stellar parameters, confirm the existence of planets, and establish the sizes and masses of the planets. Observations will be performed with committed time on the Las Cumbres Observatory Global Telescope Network and the MEarth observatory. In addition, the TESS science team members have access to numerous other facilities (e.g., Keck, Magellan, Subaru, HARPS, HARPS-North, Automated Planet Finder) through the usual telescope time allocation processes at their home institutions. The TESS team includes a large group of collaborators for follow-up observations and welcomes additional participation.

8 Anticipated Results

8.1 *Photometric Performance*

Figure 8 shows the anticipated photometric performance of the TESS cameras. The noise sources in this model are photon-counting noise from the star and the background (zodiacal light and faint unresolved stars), dark current (negligible), read-out noise, and a term representing additional systematic errors that cannot be corrected by cotrending. The most important systematic error is expected to be due to random pointing variations ("spacecraft jitter"). Because of the nonuniform quantum efficiency of the CCD pixels, motion of the star image on the CCD will introduce changes in the measured brightness, as the weighting of the image PSF changes, and as parts of the image PSF enter and exit the summed array of pixels.

The central pixel of a stellar image will saturate at approximately $I_C = 7.5$. However, this does not represent the bright limit for precise photometry because the excess charge is spread across other CCD pixels and is conserved, until the excess charge reaches the boundary of the CCD. As long as the photometric aperture is large enough to encompass all of the charge, high photometric precision can still be obtained. The Kepler mission demonstrated that photon-noise–limited photometry can be obtained for stars 4 mag brighter than the single-pixel saturation limit.[21] Since similar performance is expected for TESS, the bright limit is expected to be $I_C \approx 4$ or perhaps even brighter.

8.2 *Transit Detections*

Monte Carlo simulations are used to verify that the science objectives can be met and to anticipate the properties of the detected planetary systems.[12] These simulations are based on a model of the local neighborhood of main-sequence FGKM stars.[11] Simulated stars are populated randomly with planets, and "observed" by TESS. Those for which transits are observed with a sufficiently high signal-to-noise ratio are counted as detections. In addition, the simulated star catalog is populated with eclipsing binaries that may be blended with brighter stars to

Downloaded From: https://www.spiedigitallibrary.org/journals/Journal-of-Astronomical-Telescopes,-Instruments,-and-Systems on 12/10/2018
Terms of Use: https://www.spiedigitallibrary.org/terms-of-use

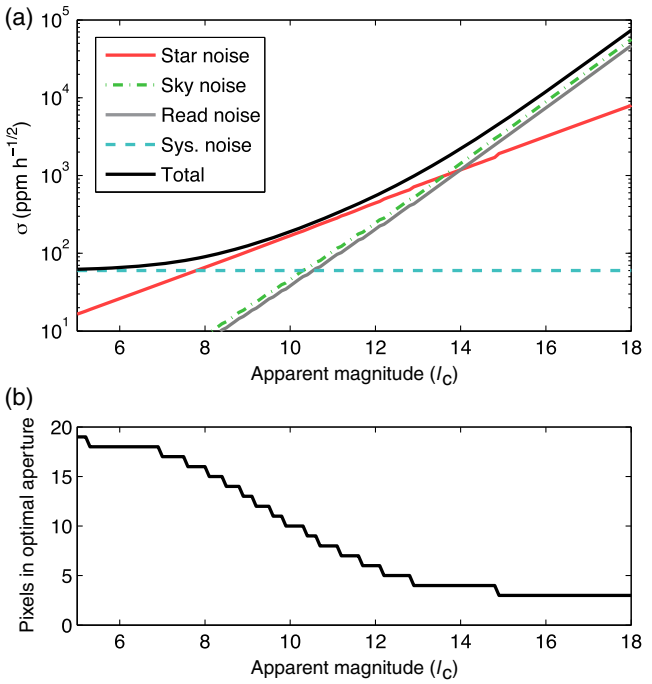

Fig. 8 (a) Expected 1σ photometric precision as a function of stellar apparent magnitude in the I_C band. Contributions are from photon-counting noise from the target star and background (zodiacal light and unresolved stars), detector read noise ($10\,e^-$), and an assumed 60 ppm of incorrigible noise on hourly timescales. (b) The number of pixels in the photometric aperture that optimizes the signal-to-noise ratio.

produce transit-like signals; the detections of these "false positives" are also recorded.

Among the features of the current simulations are: (1) a realistic distribution of stars and eclipsing binaries based on local census data; (2) probability distributions for planetary occurrence and orbital properties taken from the Kepler results;[3] (3) variation in stellar surface density and zodiacal light with position on the celestial sphere; (4) variation in the duration of TESS observations depending on ecliptic coordinates.

Figure 9 illustrates some of the results. TESS is expected to find thousands of planets smaller than Neptune, including hundreds of super-Earths ($1.25 - 2\,R_\oplus$) and tens of planets comparable in size to Earth. These will be accompanied by a comparable number of false positives (as has been the case for the Kepler mission), a majority of which are background eclipsing binaries. Some false positives will be identifiable using TESS data alone, based on the detection of secondary eclipses, ellipsoidal flux modulation, or transit-specific image motion. In other cases, ground-based observations will be required to check for composite spectra, large radial-velocity variations, color-dependent transit depths, and resolved companions that are indicative of false positives.

8.3 *Asteroseismology*

Observing photometric variations due to stellar oscillations ("asteroseismology") provides sensitive diagnostics of the stellar mass, radius, and internal dynamics. Based on the Kepler experience with mode amplitudes as a function of stellar parameters,[22] TESS can be expected to detect p-mode oscillations on about 6000 stars brighter than $V = 7.5$, including (a) the majority of all stars brighter than $V = 4.5$, (b) about 75 stars smaller than the Sun, (c) about 2000 upper-main-sequence and subgiant

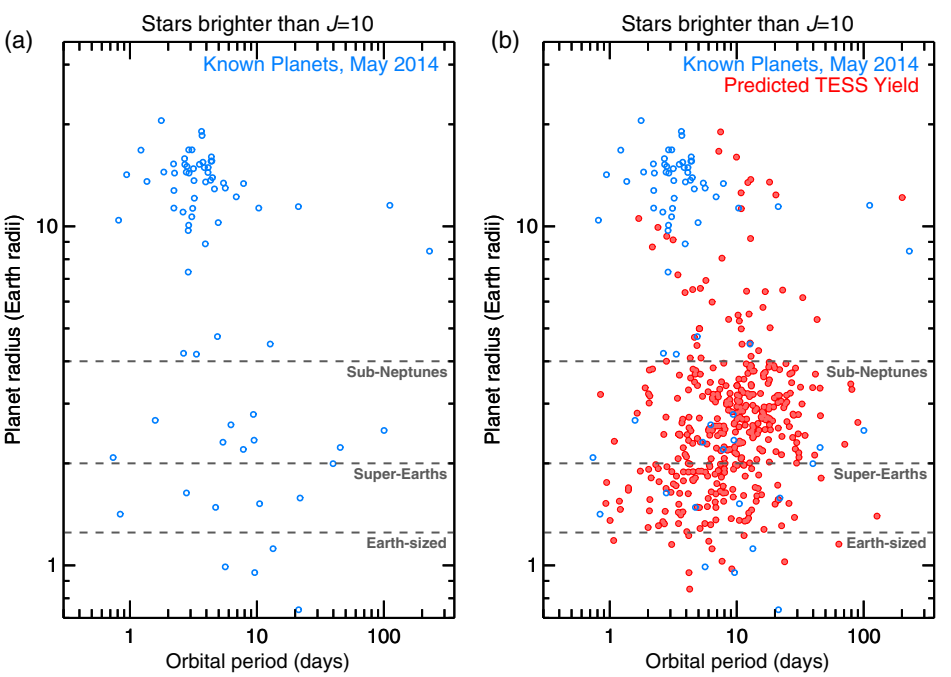

Fig. 9 Sizes and orbital periods of planets with host stars brighter than $J = 10$. The J band was chosen for convenience, since the 2MASS survey provides J magnitudes for all of the known planet-hosting stars. (a) Currently known planets, including those from the Kepler and CoRoT missions as well as ground-based surveys. (b) Including the simulated population of TESS detections.

Downloaded From: https://www.spiedigitallibrary.org/journals/Journal-of-Astronomical-Telescopes,-Instruments,-and-Systems on 12/10/2018
Terms of Use: https://www.spiedigitallibrary.org/terms-of-use

stars, and (d) virtually all the giant stars. Stars that are not suitable for planet searching but are appropriate for asteroseismology (such as giants) can be added to the TESS input catalog at minimal cost.

The key features enabling TESS's advances in this area are all-sky coverage and relatively fine time sampling. Compared to similar stars studied by CoRoT and Kepler, the TESS stars will be more numerous, brighter, and nearer to the Earth. TESS stars will have accurately known parallaxes, will be much more amenable to interferometric and radial-velocity studies, and are themselves among the likely targets for future, imaging-based missions to study exoplanets.

8.4 *Full Frame Images*

In addition to monitoring 200,000 preselected stars with a 2 min cadence, TESS will return a nearly continuous series of FFIs with an effective exposure time of 30 min. As Kepler has shown, a 30 min cadence still allows for the efficient discovery of transiting planets. The FFIs will expand the transit search to any star in the FOV that is sufficiently bright, regardless of whether it was selected ahead of time. This will reduce the impact of any imperfections in the target star catalog, and allow the search sample to extend beyond the FGKM dwarfs that are the focus of the mission. In addition, the transit candidates that are identified in the FFIs during the baseline TESS mission could be selected for shorter-cadence observations during an extended mission.

The FFIs will also enable a wide variety of other scientific investigations, such as the detection and monitoring or nearby supernovae and gamma-ray burst afterglows, bright AGN outbursts, near-Earth asteroids, eclipsing and close binaries, novae, flaring stars, and other variable stars. Each 30 min FFI will provide precise (≈5 mmag) photometry for approximately 10^6 bright galaxies and stars ($I_C < 14 - 15$) within a 2300 deg^2 field. Over 2 years, the TESS all-sky survey will provide such data for approximately 20 million bright objects, many of which will exhibit short-term variability. Thus, the TESS FFIs will provide broad-ranging fundamental data for time-domain astronomy. In particular, TESS will complement the Large Synoptic Survey Telescope, which is limited to observing objects fainter than 16th magnitude.[23]

9 Partners and their Roles

The lead institution for TESS is MIT, which hosts the principal investigator, Dr. George Ricker. The MIT Lincoln Laboratory is responsible for the cameras, including the lens assemblies, detector assemblies, lens hoods, and camera mount. NASA's Goddard Space Flight Center provides project management, systems engineering, and safety and mission assurance. Orbital Sciences Corporation (OSC) builds and operates the spacecraft. The mission is operated from the OSC Mission Operations Center.

The TESS Science Center, which analyzes the science data and organizes the coinvestigators, collaborators, and working groups (with members from many institutions) is a partnership among MIT's Physics Department and Kavli Institute for Astrophysics and Space Research, the SAO, and the NASA Ames Research Center. The raw and processed data are archived at the Mikulski Archive for Space Telescopes (MAST), at the Space Telescope Science Institute.

10 Discussion

Kepler has revealed the vast numbers of small planets that exist in the Galaxy. TESS will find them around stars in the local neighborhood, which will be easier to study with current and planned instruments, including the JWST. The TESS launch is currently scheduled for late 2017, and the all-sky survey for 2018 to 2019. An extended mission of several years is a realistic possibility, and is compatible with the supply of consumable materials and the stability of the spacecraft orbit. An extended mission would increase the number of planet detections, especially those with longer orbital periods, including planets in the habitable zones of their host stars.

A broad community effort will be needed to harvest all of the scientific potential of the survey. TESS will serve as the "People's Telescope," with a public release of the target catalog prior to launch, the first data release 6 months after launch, and subsequent data releases every 4 months, to stimulate community-wide effort and optimize target selection for subsequent studies. Light curves, full-frame images, and catalogs of "objects of interest" will be available on the MAST. The TESS team will also establish an electronic clearinghouse to exchange information and coordinate the follow-up effort.

One of the most scientifically productive—and challenging—types of follow-up observations is PRV monitoring. PRV monitoring is used to confirm the planetary nature of TESS detections, provide constraints on planetary densities and possible interior compositions, and inform the interpretation of planetary atmosphere studies with JWST and other instruments. PRV monitoring is likely to be the rate-limiting step in realizing the full benefits of TESS for exoplanetary science. Even though TESS stars are relatively bright and favorable for study, the expected number of new and interesting PRV targets will greatly exceed the time budgets of currently available observatories. Many groups are aiming to rectify this situation by building new PRV instruments. Among the new instruments being planned with TESS targets in mind are ESPRESSO,[24] NRES,[25] IRD,[26] CARMENES,[27] HPF,[28] HRS,[29] SPIRou,[30] MAROON-X,[31] CODEX,[32] and G-CLEF.[33]

The TESS legacy will be a catalog of the nearest and brightest stars hosting transiting planets, which will likely be the most favorable targets for detailed investigations in the decades or even centuries that follow.

Acknowledgments

Many people and institutions have generously supported TESS over the years, including: Aerospace Corporation, Google, the Kavli Foundation, the MIT Department of Physics, the MIT School of Science, Mr. Gregory E. Moore and Dr. Wynne Szeto, Mr. Richard M. Tavan, and Mr. Juan Carlos Torres. Extensive support has also been provided by NASA Headquarters, NASA's Goddard Space Flight Center, and NASA's Ames Research Center (ARC) under the following grants and contracts: NNG09FD65C, NNX08BA61A, NNG12FG09C, and NNG14FC03C. The authors also wish to thank the following individuals for their important scientific, technical, and other contributions to the mission: Charles Alcock, Fash Asad, Mark Bautz, Chet Beals, Dave Bearden, Marc Bernstein, Greg Berthiaume, Ed Bertschinger, Adam Burgasser, Barry Burke, Claude Canizares, Ben Cichy, Kris Clark, Dave Czajkowski, Debra Emmons, Jim Francis, Joe Gangestad, Bob Goeke, Jose Guzman, Kari Haworth, Greg Henning, Jackie Hewitt, Shane Hynes, Marc Kastner, Brian

Downloaded From: https://www.spiedigitallibrary.org/journals/Journal-of-Astronomical-Telescopes,-Instruments,-and-Systems on 12/10/2018
Terms of Use: https://www.spiedigitallibrary.org/terms-of-use

Lewis, Robert Lockwood, Gerry Luppino, Francois Martel, Bill Mayer, Chad Mendelsohn, Ed Morgan, Bill Oegerle, Randy Persinger, Ron Remillard, Matt Ritsko, Tim Sauerwein, Robbie Schingler, Joe Scillieri, Rob Simcoe, Tony Smith, Dave Strobel, Vyshi Suntharalingam, Jeff Volosin, Kim Wagenbach, Nick White, Pete Worden, and Maria Zuber.

References

1. J. N. Winn, "Exoplanet transits and occultations," in *Exoplanets*, S. Seager, Ed., pp. 55–77, University of Arizona Press, Tucson, Arizona (2011).
2. W. J. Borucki et al., "Characteristics of planetary candidates observed by Kepler. II. Analysis of the first four months of data," *Astrophys. J.* **736**(1), 19 (2011).
3. F. Fressin et al., "The false positive rate of Kepler and the occurrence of planets," *Astrophys. J.* **766**(2), 81 (2013).
4. G. W. Marcy et al., "Masses, radii, and orbits of small Kepler planets: the transition from gaseous to rocky planets," *Astrophys. J. Suppl. Ser.* **210**(2), 20 (2014).
5. J. J. Lissauer et al., "Architecture and dynamics of Kepler's candidate multiple transiting planet systems," *Astrophys. J. Suppl. Ser.* **197**(1), 8 (2011).
6. G. R. Ricker et al., "The high energy transient explorer (HETE): mission and science overview," in *Gamma-Ray Burst and Afterglow Astronomy 2001: A Workshop Celebrating the First Year of the HETE Mission*, G. R. Ricker and R. K. Vanderspek, Eds., Vol. 662, pp. 3–16, American Institute of Physics, Melville, NY (2003).
7. J. Pepper, A. Gould, and D. L. Depoy, "Using all-sky surveys to find planetary transits," *Acta Astron.* **53**, 213–228 (2003).
8. B. S. Gaudi, S. Seager, and G. Mallen-Ornelas, "On the period distribution of close-in extrasolar giant planets," *Astrophys. J.* **623**(1), 472–481 (2005).
9. J. P. Gardner et al., "The James Webb Space Telescope," *Space Sci. Rev.* **123**(4), 485–606 (2006).
10. D. Charbonneau et al., "A super-Earth transiting a nearby low-mass star," *Nature* **462**, 891–894 (2009).
11. L. Girardi et al., "Star counts in the galaxy. Simulating from very deep to very shallow photometric surveys with the trilegal code," *Astron. Astrophys.* **436**(3), 895–915 (2005).
12. P. Sullivan et al., "The Transiting Exoplanet Survey Satellite: simulated planet detections," *Astrophys. J.*, in preparation (2014).
13. R. Gilliland et al., "Kepler mission stellar and instrument noise properties," *Astrophys. J. Suppl. Ser.* **197**(1), 6 (2011).
14. J. W. Gangestad et al., "A high Earth, lunar resonant orbit for lower cost space science missions," *Adv. Astron. Sci.* **150**, 13–810 (2014).
15. M. F. Skrutskie et al., "The two micron all sky survey (2MASS)," *Astron. J.* **131**(2), 1163–1183 (2006).
16. E. Høg et al., "The Tycho-2 catalogue of the 2.5 million brightest stars," *Astron. Astrophys.* **355**, L27–L30 (2000).
17. N. Zacharias et al., "The fourth US naval observatory CCD astrograph catalog (UCAC4)," *Astron. J.* **145**(2), 44 (2013).
18. M. S. Bessell and J. M. Brett, "JHKLM photometry—standard systems, passbands, and intrinsic colors," *Publ. Astron. Soc. Pac.* **100**, 1134–1151 (1988).
19. S. Salim and A. Gould, "Classifying Luyten stars using an optical-infrared reduced proper-motion diagram," *Astrophys. J. Lett.* **575**(2), L83–L86 (2002).
20. J. M. Jenkins et al., "Overview of the Kepler science processing pipeline," *Astrophys. J. Lett.* **713**(2), L87–L91 (2010).
21. R. Gilliland et al., "Initial characteristics of Kepler short cadence data," *Astrophys. J. Lett.* **713**(2), L160–L163 (2010).
22. W. J. Chaplin et al., "The asteroseismic potential of Kepler: first results for solar-type stars," *Astrophys. J. Lett.* **713**(2), L169–L175 (2010).
23. LSST Science Collaborations and LSST Project, *LSST Science Book*, Version 2.0, arXiv:0912.0201, LSST Corporation, Tucson, AZ, http://www.lsst.org/lsst/scibook (2009).
24. F. Pepe et al., "ESPRESSO: the Echelle spectrograph for rocky exoplanets and stable spectroscopic observations," *Proc. SPIE* **7735**, 77350F (2010).
25. J. Eastman et al., "NRES: the network of robotic Echelle spectrographs," *Proc. SPIE* **9147**, 914716 (2014).
26. M. Tamura et al., "Infrared Doppler instrument for the Subaru Telescope (IRD)," *Proc. SPIE* **8446**, 84461T (2012).
27. A. Quirrenbach et al., "CARMENES: Calar alto high-resolution search for M dwarfs with exo-Earths with a near-infrared Echelle spectrograph," *Proc. SPIE* **7735**, 773513 (2010).
28. S. Mahadevan et al., "The habitable-zone planet finder: a stabilized fiber-fed NIR spectrograph for the Hobby-Eberly telescope," *Proc. SPIE* **8446**, 84461S (2012).
29. D. Bramall et al., "The SALT HRS spectrograph: instrument integration and laboratory test results," *Proc. SPIE* **8446**, 84460A (2012).
30. X. Delfosse et al., "World-leading science with SPIRou—the NIR spectropolarimeter/high-precision velocimeter for CFHT," in *Conf. Proc. of the French Society of Astronomy and Astrophysics Meeting*, L. Cambresy, Eds., pp. 497–508, French Astronomical Society, Paris, France (2013).
31. J. Bean, University of Chicago, Chicago, IL, United States, private communication, astro.uchicago.edu/~jbean/spectrograph.html (2014).
32. L. Pasquini et al., "CODEX: the high-resolution visual spectrograph for the E-ELT," *Proc. SPIE* **7014**, 70141I (2008).
33. A. Szentgyorgyi et al., "The GMT-CfA, Carnegie, Catolica, Chicago Large Earth Finder (G-CLEF): a general purpose optical Echelle spectrograph for the GMT with precision radial velocity capability," *Proc. SPIE* **8446**, 84461H (2012).

George R. Ricker is the PI for the Transiting Exoplanet Survey Satellite mission. He is a senior research scientist and director of the CCD Laboratory at the MIT Kavli Institute. He was the PI for the HETE mission (launched in 2000), PI for the CCD x-ray camera on the ASCA mission (1993), deputy-PI for the Chandra ACIS Instrument (1999), and the US PI for the x-ray CCD camera on the Astro-E1 mission.

Biographies of the other authors are not available.

Downloaded From: https://www.spiedigitallibrary.org/journals/Journal-of-Astronomical-Telescopes,-Instruments,-and-Systems on 12/10/2018
Terms of Use: https://www.spiedigitallibrary.org/terms-of-use